The Journal of Experimental Biology 212, 2835-2843
Published by The Company of Biologists 2009
doi:10.1242/jeb.029975

Surface tension propulsion of fungal spores

Xavier Noblin[1], Sylvia Yang[2] and Jacques Dumais[3,*]

[1]Laboratoire de Physique de la Matière Condensée, CNRS –UMR 6622, Université de Nice-Sophia-Antipolis, Parc Valrose, 06108 Nice, Cedex 2, France, [2]Department of Biology, University of Washington, Seattle, WA 98195, USA and [3]Department of Organismic and Evolutionary Biology, Harvard University, Cambridge, MA 02138, USA

*Author for correspondence (jdumais@oeb.harvard.edu)

Accepted 6 June 2009

SUMMARY

Most basidiomycete fungi actively eject their spores. The process begins with the condensation of a water droplet at the base of the spore. The fusion of the droplet onto the spore creates a momentum that propels the spore forward. The use of surface tension for spore ejection offers a new paradigm to perform work at small length scales. However, this mechanism of force generation remains poorly understood. To elucidate how fungal spores make effective use of surface tension, we performed a detailed mechanical analysis of the three stages of spore ejection: the transfer of energy from the drop to the spore, the work of fracture required to release the spore from its supporting structure and the kinetic energy of the spore after ejection. High-speed video imaging of spore ejection in *Auricularia auricula* and *Sporobolomyces* yeasts revealed that drop coalescence takes place over a short distance (~5 μm) and energy transfer is completed in less than 4 μs. Based on these observations, we developed an explicit relation for the conversion of surface energy into kinetic energy during the coalescence process. The relation was validated with a simple artificial system and shown to predict the initial spore velocity accurately (predicted velocity: 1.2 m s^{-1}; observed velocity: 0.8 m s^{-1} for *A. auricula*). Using calibrated microcantilevers, we also demonstrate that the work required to detach the spore from the supporting sterigma represents only a small fraction of the total energy available for spore ejection. Finally, our observations of this unique discharge mechanism reveal a surprising similarity with the mechanics of jumping in animals.

Supplementary material available online at http://jeb.biologists.org/cgi/content/full/212/17/2835/DC1

Key words: *Auricularia auricula*, ballistospores, wetting phenomena, spore dispersal, surface tension.

INTRODUCTION

Most basidiomycetes, including many edible mushrooms, actively disperse their spores through a mechanism known as ballistospory (Buller, 1909-1950; Ingold, 1939). The spores, or ballistospores, are borne on the gills of mushroom caps or equivalent reproductive structures (Fig. 1A). Each spore develops on an outgrowth known as the sterigma to which it is attached *via* the hilum – a constriction of the sterigma that works as an abscission zone (Fig. 1B,C). Spore ejection is preceded by the condensation of Buller's drop at the hilar appendix located on the proximal end of the spore (Fig. 1D,E). Buller's drop is nucleated by the secretion of hygroscopic substances (such as mannitol) that decrease the vapor pressure of the incipient droplet (Webster et al., 1995). In the meantime, a film of water develops on the spore probably following a similar process. When the drop reaches a critical size, it touches the water film on the spore surface. At this point, surface tension quickly pulls the drop onto the spore thus creating the necessary momentum to detach the spore from the sporogenic surface. The spore can then fall freely under the action of gravity. Upon emerging from the cap, the spore is carried away by air currents to a distant location where it can germinate to produce a new mycelium and, ultimately, new mushrooms.

Surface tension is almost imperceptible at length scales at which humans operate. However, at microscopic length scales, surface tension forces dominate over the force of gravity. This fact can be understood from a simple scaling argument. The force of gravity on an object such as a spore scales as $F_g \sim \rho g R^{-3}$, where ρ is the density of the object, g=9.8 m s^{-2} is the gravitational acceleration and R is the characteristic length of the object. By contrast, the surface tension force is $F_\gamma \sim \gamma R$, where γ is the liquid's surface tension ($\gamma = 72 \times 10^{-3}$ N m^{-1} for water at room temperature). Considering the ratio of these forces: $F_\gamma / F_g \sim \gamma / \rho g R^2$; it can be seen that as R gets small, the surface tension force becomes increasingly important and dominates the force of gravity for R smaller than 1 mm. This simple phenomenon has profound consequences on the release of spores. The dispersal of most fungal spores by wind requires that the spores be small thus making the force of gravity inconsequential compared with adhesion forces. As a result, spores tend to cling to each other and to the gills of mushroom caps. Active spore ejection provides a solution to this problem, which explains the great diversity of mechanisms for spore release in fungi and nonvascular plants (Straka, 1962). However, unlike other active dispersal mechanisms, which involve mass release of spores from specialized launching structures, ballistospores are self-propelled by water.

Given that a large mushroom can shed spores at the astonishing rate of 40 million spores per hour (Buller, 1909-1950); the release of ballistospores has rightfully attracted some attention (Buller, 1909-1950; Ingold, 1939; Money, 1998). As early as 1939, Ingold determined that the surface energy in Buller's drop is sufficient to account for the kinetic energy of the spore (Ingold, 1939). He, however, concluded his discussion of the topic remarking that 'although there appears to be sufficient surface energy to discharge the spore it is not too easy to see how this energy could be mobilized to bring about discharge' (Ingold, 1939). More recently, Turner and

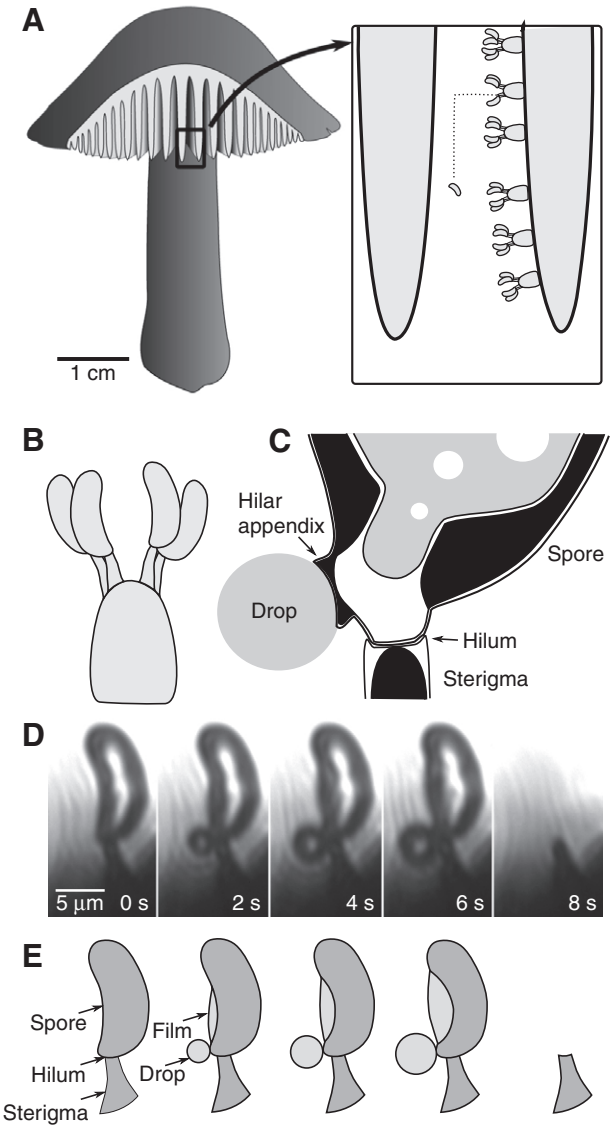

Fig. 1. Ballistospore discharge in basidiomycetes. (A) Section of a typical mushroom cap showing the gills and the location of the spore-bearing basidia (insert). The approximate trajectory of the spore is shown as a broken line. (B) A typical basidium with four spores. (C) Structure of the lower half of the spore [based on McLaughlin et al. (McLaughlin et al., 1985)]. (D) Spore ejection in *Auricularia auricula*. In this species, spores are borne singly on the sporogenic surfaces. (E) Diagrammatic representation of the ejection in D.

Webster (Turner and Webster, 1991) were able to predict the initial spore velocity with respectable accuracy based on a few judicious assumptions. The development of high-speed video cameras and their recent application to visualize ballistospore ejection (Pringle et al., 2005) provide, for the first time, a way to address Ingold's question with direct measurement of all key parameters in the problem.

Here, we present a detailed analysis of how surface tension is used for spore ejection in *Auricularia auricula* ('tree ears') and *Sporobolomyces* yeasts. In particular, we quantify the forces and energies of the three stages of the ejection process: the transfer of surface energy from the drop to the spore, the work of fracture required to release the spore from the sterigma and the kinetic energy of the spore after ejection. Our analysis reveals an exquisite fine-tuning of the different stages that yields a surprisingly high efficiency for the transfer of energy from Buller's drop to the spore.

MATERIALS AND METHODS

Specimen preparation

To initiate spore development and spore discharge, dehydrated *Auricularia auricula* (Fr.) J. Schrot fragments were first imbibed on a wet towel and then kept under humid conditions with the fertile surface facing downward. After a few hours, spore ejection had begun as indicated by the presence of white spores on the bottom of the dish. We cut thin vertical sections (0.5 mm) of the fungus and laid them flat on a microscope slide covered with a thin (100–200 μm) layer of 2% agar. Sterigmas were now oriented horizontally so that spores were ejected perpendicular to the optical axis of the microscope. Spores from yeast-like species were isolated from leaves. Although the yeasts were not identified to the species level, they are members of the Urediniomycetes (the rust fungi), likely to be of the genus *Sporobolomyces*. The yeasts were plated from a primary culture onto a thin layer of a 2% nutrient agar. After a few days, the spores germinated to form hyphae, sterigmas and new spores. Our yeast cultures may have included more than one species but we found little quantitative differences between the different cultures. Therefore, for simplicity, we are treating all samples as a single taxon. All experiments were performed on *A. auricula* and the yeast species, except for the work of fracture of the hilum, which was performed on *A. auricula* only.

Microscopy and imaging

All imaging was done in transmitted light with ×20 and ×40 objectives. Images were captured with a Phantom V7.0 (Wayne, NJ, USA) or a Photron Ultima APX-RS (San Diego, CA, USA) high-speed camera at a frame rate of up to 250,000 frames s^{-1} and exposure times as short as 1 μs. The high acquisition rate necessary to capture spore ejection can be achieved only when image resolution is low (typically 32×128 pixels). Although our analyses were performed on these raw images, the frames from the time-lapse sequences are presented in the figures at higher resolution to improve clarity. We include as supplementary material three movies (AVI format) for *A. auricula* and one for the *Sporobolomyces* yeasts (see Movies 1–4 in supplementary material). The frame rates for Movies 1–4 are, respectively 90,000 frames s^{-1}; 80,000 frames s^{-1}; 250,000 frames s^{-1}; 90,000 frames s^{-1}.

Spore ballistics

We developed image analysis routines in Matlab (The MathWorks, Natick, MA, USA) to track the centroid of the spore and the rotation of the spore's major axis over the entire trajectory. Although spore translation in *A. auricula* and *Sporobolomyces* yeasts could be tracked reliably in all time-lapse sequences, only *A. auricula* offered two spores with rotation confined to the imaging plane that could thus be analyzed for their angular velocity. The *Sporobolomyces* yeasts could not be positioned such that the spore trajectory was confined to the focal plane of the microscope; the spores thus moved quickly out of focus. To compute the spore velocity, we used a 3-D tracking algorithm that relies on the size of the out-of-focus spore to infer its vertical position. The calibration for the vertical position was obtained by imaging particles at known vertical displacements above or below the focal plane and recording the size of the out-of-focus particles.

As we shall show in the Results section, the Reynolds number (*Re*) for spore ejection is small. Therefore Stokes' law provides a good description of the drag force acting on the spore (Happel and

Brenner, 1983). Assuming a spherical spore, the ballistic trajectory of the spore will thus be governed by the following force balance: $D=6\pi\mu Rv=ma$, where D is the drag force, R, m, v and a are, respectively, the mean radius, mass, velocity and acceleration of the spore (including the fused drop), and $\mu=1.84\times10^{-5}$ Pa s is the dynamic viscosity of air. The force balance equation can be rearranged to give:

$$\frac{1}{v}\frac{dv}{dt}=\frac{6\pi\mu R}{m}\,. \quad (1)$$

Integrating gives $v(t)=V_0\exp(-t/\tau_T)$, where the characteristic decay time associated with the translational velocity $\tau_T=m/6\pi\mu R$ and V_0 is the initial velocity of the spore. We can integrate again to find the spore position along the axis of discharge (x) assuming that $x(0)=0$:

$$x(t)=V_0\tau_T(1-e^{-t/\tau_T}). \quad (2)$$

A similar equation can be derived for the viscous dissipation associated with the rotation of the spore:

$$\alpha(t)=\Omega_0\tau_R(1-e^{-t/\tau_R}), \quad (3)$$

where α is the angular position of the spore, Ω_0 is the initial angular velocity and $\tau_R=m/20\pi\mu R$ is the characteristic decay time for the rotation of the spore (Happel and Brenner, 1983). Eqns 2 and 3 were used to fit the observed spore trajectories and infer the parameters V_0, Ω_0, τ_T and τ_R.

Measurement of rupture force

The rupture force of the hilum in *A. auricula* was measured with custom-made micropipettes calibrated on an analytical balance (0.1 μN precision). Using a micromanipulator, a micropipette was brought into contact with the top of the spore, perpendicular to the sterigma. A water film provided adhesion between the spore and the glass micropipette. In some experiments, we also used poly-L-lysine-coated micropipettes to enhance adhesion. The micropipette was then displaced slowly until the spore detached from the sterigma or until the adhesion between the spore and pipette failed. The force was calculated from the deflection of the micropipette with an error of ±5%. To infer the spring constant of the sterigma, we measured its elongation δ just prior rupture (error of 10%).

Surface energy available for spore ejection

The energy available to eject the spore comes from the surface energy stored in Buller's drop. For *A. auricula*, the surface energy freed during the fusion process (ΔE_p) can be calculated from the coalescence of a spherical drop onto a plane (Fig. 2A). The energy is equal to the difference in surface area of the spore–drop system before and after coalescence, i.e.:

$$\Delta E_p=(\gamma_{SV}A_S+\gamma 4\pi R_D^2)-(\gamma_{SL}A_S+\gamma A_D)=(\gamma_{SV}-\gamma_{SL})A_S+\gamma(4\pi R_D^2-A_D), \quad (4)$$

where γ_{SV}, γ_{SL} and γ are the energies associated with the spore–vapor, spore–liquid and liquid–vapor interfaces, respectively. R_D is the radius of the drop before fusion, A_S is the area of the spore covered by the drop after fusion and A_D is the drop surface area after fusion.

Using Young's law for the contact angle ($\gamma_{SV}=\gamma_{SL}+\gamma\cos\theta$) (de Gennes et al., 2003), we have:

$$\Delta E_p=\gamma(\cos\theta A_S-A_D+4\pi R_D^2). \quad (5)$$

The coalesced drop is a spherical cap of radius R'_D and contact angle θ for which the area is $A_D=2\pi R_D'^2(1-\cos\theta)$, the volume is $\pi R_D'^3(1-\cos\theta+(\cos^3\theta-1)/3)$ and the projected area onto the spore is $A_S=\pi(R'_D\sin\theta)^2=\pi R_D'^2(1-\cos^2\theta)$. Then:

$$\gamma(A_S\cos\theta-A_D)=\gamma(\pi R_D'^2\cos\theta(1-\cos^2\theta)-2\pi R_D'^2(1-\cos\theta))=-\gamma\pi R_D'^2(2-3\cos\theta+\cos^3\theta). \quad (6)$$

From the conservation of the volume, one can write:

$$4/3\,\pi R_D^3=\pi/3R_D'^3(2-3\cos\theta+\cos^3\theta). \quad (7)$$

Therefore, the surface energy available for spore ejection is:

$$\Delta E_p=\gamma 4\pi R_D^2(1-R_D/R'_D). \quad (8)$$

As would be expected, ΔE_p is proportional to the total surface area of Buller's drop ($4\pi R_D^2$) times a factor that accounts for the degree of spreading of the drop onto the spore ($1-R_D/R'_D$). The surface energy for the nearly spherical spores of the *Sporobolomyces* is easy to derive assuming that Buller's drop envelops the spore (Fig. 2B).

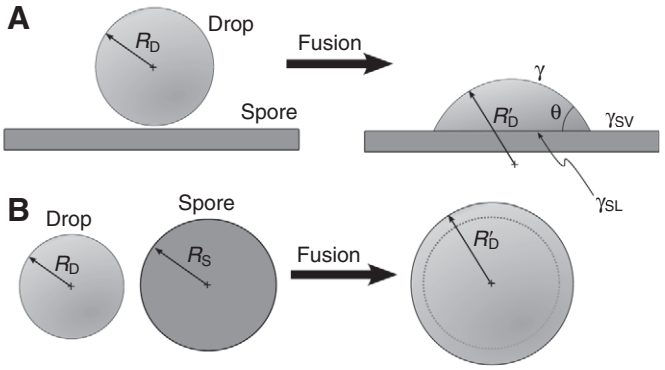

Fig. 2. (A) Spore and drop geometry for *Auricularia auricula*. (B) Spore and drop geometry for the *Sporobolomyces* yeasts. R_D, R'_D, radius of the drop before and after fusion, respectively. R_S, spore radius; γ, γ_{SL}, γ_{SV}, surface tension for the liquid–vapor interface, solid–liquid interface, and solid–vapor interface. θ, contact angle.

Error analysis

The main error in our experimental observations comes from the length measurements made on video images. These measurements are used to assess the spore and drop radii and for calculating their volumes. The length measurements were precise to ±0.5 pixels whereas the diameter of the drop was <7 pixels and the spore's dimensions were ~8×15 pixels. As seen in Eqn 8, the prediction of the freed surface energy depends on two length measurements: R_D and R'_D. Prediction of the initial spore velocity V_0 requires in addition the width (W_S) and length (L_S) of the spore. The absolute error on the velocity estimate (ΔV_0) is given by the following equation:

$$\Delta V_0=\left|\frac{\partial V_0}{\partial R_D}\right|\Delta R_D+\left|\frac{\partial V_0}{\partial R'_D}\right|\Delta R'_D+\left|\frac{\partial V_0}{\partial W_S}\right|\Delta W_S+\left|\frac{\partial V_0}{\partial L_S}\right|\Delta L_S\,, \quad (9)$$

where $\Delta R_D=\Delta R'_D=\Delta W_S=\Delta L_S=0.5$ pixels are the absolute errors for the length measurements. Using Eqn 9, we find that the relative error on the predicted velocity is $\Delta V_0/V_0=22\%$.

RESULTS

Spore ejection is best described by first analyzing the spore ballistics to infer the spore initial velocity and kinetic energy. We then proceed to a mechanical analysis of the stages that precede ejection.

Spore ballistics – the 'sporabola'

To quantify the initial velocity and kinetic energy present in the spore at the moment of ejection, we analyzed the ballistic trajectory of the spore (Figs 3 and 4; Movies 1–4 in supplementary material). Buller coined the word 'sporabola' to describe the particular trajectory followed by the spore (Buller, 1909-1950). The shape of the sporabola results from the interplay of gravity and viscous forces acting on the spore. The Reynolds number at ejection is $Re=V_0L_S/\nu\approx0.5$, where ν is the kinematic viscosity of air ($1.4\times10^{-3}\,m^2\,s^{-1}$). Given the small Reynolds number, Stokes' law provides a good description of the drag force acting on the spore (Happel and Brenner, 1983). The spore position along the axis of discharge x is thus given by (see Materials and methods section):

$$x(t) = V_0\tau_T\,(1 - e^{-t/\tau_T}). \quad (10)$$

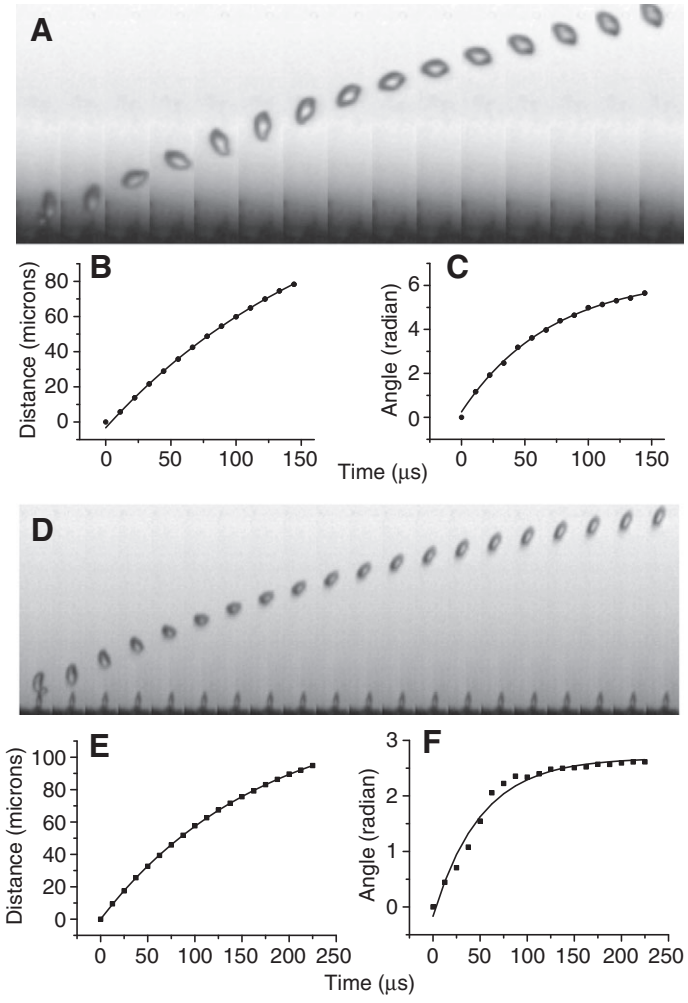

Fig. 3. Spore ballistics in *Auricularia auricula*. (A) Spore trajectory (frame rate: 90,000 frames s^{-1}, shutter: 2 μs) (see Movie 1 in supplementary material). Spore position (B) and rotation angle (C) *versus* time for the sequence shown in A. The data points are fitted with the kinematic equations derived from Stokes' Law. (D) Spore trajectory (frame rate: 80,000 frames s^{-1}, shutter: 2 μs) (see Movie 2 in supplementary material). Spore position (E) and rotation angle (F) *versus* time. As above, the data points are fitted with the kinematic equations derived from Stokes' Law. In this example, the rotation of the spore is not fully confined to the imaging plane, which explains the slight deviation of the observed angular position from the theory (F).

The spore rotation, clearly seen in Fig. 3A,D, is also damped by air viscosity. The angular position is:

$$\alpha(t) = \Omega_0\tau_R\,(1 - e^{-t/\tau_R}). \quad (11)$$

As shown in Fig. 3, these relationships fit the data very well and yield, for the spore shown in Fig. 3A, an initial velocity of $V_0=0.8\,m\,s^{-1}$, an angular velocity of $\Omega_0=9\times10^4\,rad\,s^{-1}$ and decay times of $\tau_T=184\,\mu s$ and $\tau_R=66\,\mu s$ (see Table 1 for a summary of the data). Fig. 4 shows spore ejection in a *Sporobolomyces* yeast. For this sequence, the spore velocity is $V_0=1.6\,m\,s^{-1}$.

According to Stokes' law, the decay times are $\tau_T=m_{SD}/6\pi\mu R$ and $\tau_R=m_{SD}/20\pi\mu R$, where R and m_{SD} are, respectively, the mean radius and mass of the spore–drop complex (see Materials and methods) (Happel and Brenner, 1983). We can therefore compare the decay times inferred from the fitted spore displacement in Fig. 3 with those predicted by the theory. For the decay time associated with the translational velocity (τ_T), the mean ratio of the measured over the predicted decay times is 0.91 (standard deviation: $\sigma=0.08$, for $N=4$ measurements). For the decay time associated with the angular velocity (τ_R), the average ratio is 1.08 ($\sigma=0.19$, $N=2$). The measurements are therefore in surprising close agreement with the theory.

Finally, we can look at the kinetic energy of the spore. The translational energy is $E_K=m_{SD}V_0^2/2$ and the rotational energy is $E_R=m_{SD}r_g^2\Omega_0^2/2$, where r_g is the spore's radius of gyration. The radius of gyration for a prolate spore rotating about its short axis is $r_g=(a^2+b^2)/5$, where a and b are the minor and major semi-axes of the spheroid. Substituting values for the sequences shown in Fig. 3, we find $E_K=2.3\times10^{-13}$ J and $E_R=6.3\times10^{-15}$ J. Therefore, the amount of energy transferred into translation of the spore is at least 30 times greater than the energy associated with the spore's rotation.

Ejection model

We now address the most fundamental question of the ejection mechanism – how the surface energy stored in Buller's drop is transformed into kinetic energy. To answer this question, we need a proper understanding of the fusion process. Fusion takes place over a time interval of less than 4 μs and is therefore just below the temporal resolution of most high-speed cameras currently available. Using a frame rate of 250,000 images per second and a shutter speed of 1 μs, we obtained some new and critical information about the early stages of spore ejection (Fig. 5). The first frame in Fig. 5A shows the drop that has condensed at the

Table 1. Summary of key measurements

Parameter*	*Auricularia*	*Sporobolomyces*
Spore		
Mass (m_S)	2.8×10^{-13} kg	1.5×10^{-13} kg
Radius of gyration (r_g)	3.1 μm	2.2 μm
Translational velocity (V_0)	0.8 m s^{-1}	2.3 m s^{-1}
Angular velocity (Ω_0)	7.1×10^4 rad s^{-1}	NA
Translational kinetic energy (E_K)	2.3×10^{-13} J	6.7×10^{-13} J
Rotational kinetic energy (E_R)	6.3×10^{-15} J	NA
Rupture force (F_B)	0.15 μN	NA
Drop		
Mass (m_D)	4.9×10^{-14} kg	1.2×10^{-13} kg
Radius (R_D)	2.25 μm	3 μm
Final radius (R'_D)	5.65 μm	NA

*All means are based on at least five replicates except for the angular velocity and the rotational kinetic energy, which are based on two measurements.

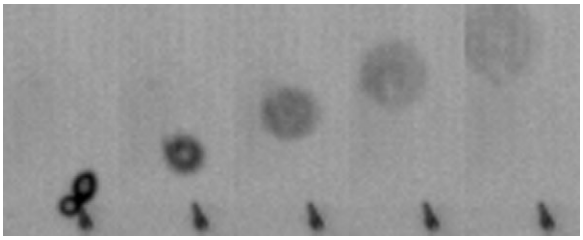

Fig. 4. Spore ejection in a *Sporobolomyces* yeast (see Movie 4 in supplementary material). In the first frame, the drop is seen to the left of the spore.

base of the spore. On the second frame, the drop has touched the spore and coalesced. The drop has not spread over the spore completely because its outline can still be discerned. In the third frame, the spore has been ejected while the top border of the drop is still visible on the spore. Finally, the last frame shows the spore rotation in and out of the image plane. This sequence of images establishes that the drop travels only a short distance on the spore and does not spread over the entire surface. Fig. 5B,C offers additional evidence of the partial fusion of the drop, which, as we will show, has some important implications for the amount of surface energy available to release the spore.

Consideration of the forces acting during the coalescence of Buller's drop reveals that ballistospore ejection is the fungal equivalent of jumping (Fig. 6). The same three ingredients are present – a lowering of the center of mass, a quick release of energy and an interaction with a rigid support. Growth of Buller's drop at the proximal end of the spore lowers the spore's center of mass (i.e. it brings it closer to the sterigma) as well as provides the energy to be used during ejection. This step is the ballistospore's way of bending its 'legs' in preparation for jumping. As soon as fusion begins, the drop exerts on the spore a surface tension force directed towards itself and the spore exerts on the drop a force of the same

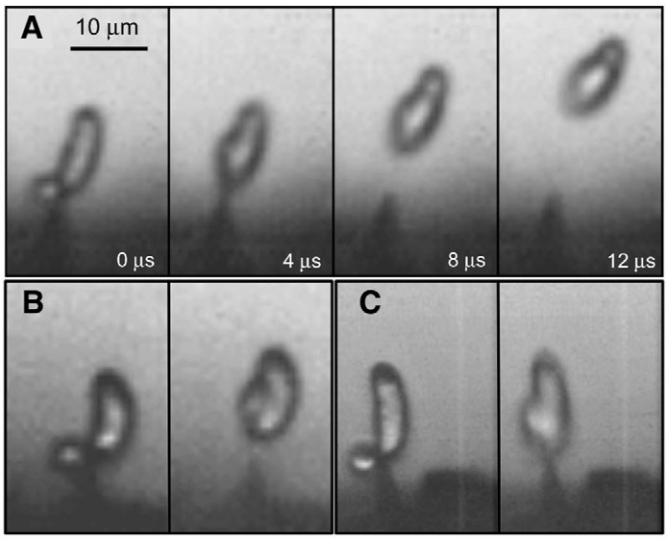

Fig. 5. Early stages of spore discharge in *Auricularia auricula*. It can be seen from these frames that the drop does not spread completely over the spore (see also Movie 3 in supplementary material). The frame rates and shutter times are, respectively: (A) 250,000 frames s^{-1} and 1 μs; (B) 100,000 frames s^{-1} and 2 μs; (C) 75,000 frames s^{-1} and 4 μs.

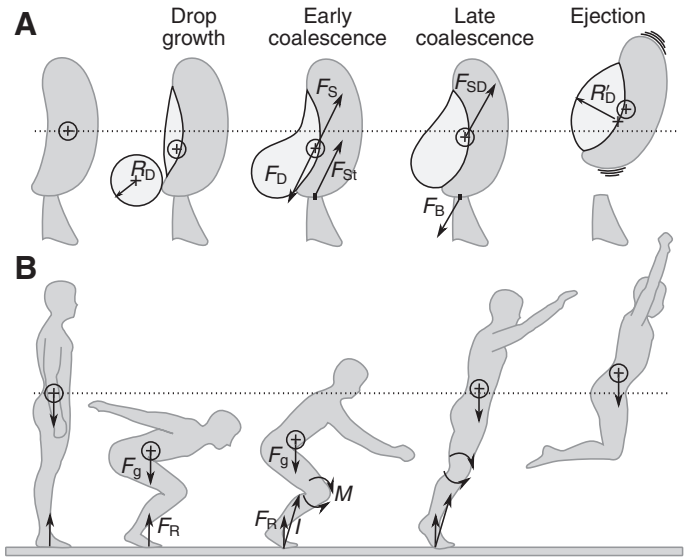

Fig. 6. (A) The four stages of ballistospore ejection. First, the growth of the drop brings the center of mass of the spore–drop complex closer to the end of the sterigma. Second, at the start of the coalescence process, the drop and spore exerts on it each other forces of equal magnitude but opposite direction (F_D and F_S). The expected downward displacement of the spore is prevented by the presence of the sterigma, giving rise to a reaction force F_{St} acting at the hilum. Third, in late coalescence, the momentum of the drop is transferred to the spore, which was immobile until then. The transfer of momentum is equivalent to a force F_{SD} applied at the center of mass of the spore–drop complex. This force puts the hilum under tension, which provides a counteracting force that cannot exceed the fracture force (F_B). Fourth, the hilum is fractured; thus, releasing the spore. (B) The corresponding stages in jumping. First, the center of mass is lowered to allow the legs to do work on the substratum. At this stage, the gravitational force (F_g) and the ground reaction force (F_R) are balanced. Second, as the legs unfold, the moments at the joints (M) are resisted by the substratum thus providing the impulse (I) necessary to accelerate the center of mass. Third, late in the jump, the fast-moving upper body starts to entrain the legs, which to this point were moving slowing upward. Fourth, after take-off all body parts are moving at similar speeds and only gravity acts on the body.

magnitude but of opposite direction (Fig. 6A). With no external interaction (isolated system), the drop and spore would move towards each other, and the global center of mass would remain immobile. Thus, there would be no ejection. In the case of ballistospores, the sterigma plays the role of the rigid support. Its presence prevents the spore from moving towards the drop by exerting a reaction force opposing the surface tension force applied by the drop. The sterigma force is the external force acting on the spore–drop complex that leads to the motion of the center of mass. The same requirement for interaction with a rigid support is found in jumping. There, the moments applied at the leg joints must be resisted by the ground to generate the impulse that will accelerate the center of mass. Ballistospore ejection, however, differs from jumping in one important way. The spore is not resting on the sterigma but is attached to it. Therefore, as the spore launches forward, it will put the sterigma under tension. The latter must break easily to release the spore.

This scenario emphasizes the critical role played by Buller's drop and the sterigma during spore ejection. We can subdivide the ejection process into four stages (Fig. 6). During the first stage, Buller's drop grows thus lowering the center of mass of the spore and storing the

energy that will be used during ejection. The second stage encompasses the early coalescence during which the sterigma is under compression and provides the counter-acting force necessary to move the global center of mass of the spore–drop complex. It is this force that allows Buller's drop to be accelerated up to a characteristic speed V_D. In the third phase, the drop decelerates as it transfers its momentum to the spore. The sterigma is now under tension and needs to break easily to release the spore without dissipating its kinetic energy. Finally, the fourth stage is the release of the spore.

The simplest model for energy transfer suggests that the kinetic energy of the drop is equal to the difference in surface energy, ΔE_p, between the initial state just before coalescence and the final state just after coalescence (energy loss will be considered in the last section). The validity of this assumption can be ascertained by estimating the Reynolds number for the drop motion. We find $Re=V_D R_D/\nu \approx 50$. The relatively large value for the Reynolds number confirms that viscous effects are small compared with inertial effects, leading to an efficient transfer of surface energy into kinetic energy. Therefore, we can write $m_D V_D^2/2=\Delta E_p$, where m_D and V_D are the mass and velocity of the drop, respectively. The latter phase of the coalescence is an inelastic shock between the drop and the spore. Although the energy is not conserved, the linear momentum is conserved which implies that $V_0=m_D V_D/m_{SD}$. This model answers Ingold's question of how the surface energy stored in Buller's drop is transformed into kinetic energy of the spore.

Rupture force of the sterigma

The strength of the chitinous wall of the sterigma could easily exceed the force created by the fusion of Buller's drop. Therefore, to predict the initial velocity of the spore at ejection, the energy required to break the hilum must be known. We measured the rupture force (F_B) by pulling on spores with calibrated glass microcantilevers. The microcantilever was brought in contact with the distal end of the spore and gradually pulled away (Fig. 7, insets). Surface tension between the cantilever and the spore allowed us to put the spore and sterigma under tension. Our measurements reveal two spore classes (Fig. 7). Some spores are weakly attached to the sterigma and are removed with a force between 0.08 and 0.3 μN (mean F_B=0.15 μN). Other spores are strongly attached to the sterigma and cannot be removed with forces up to 1.2 μN (the maximal force that could be applied with the experimental set-up). For these spores, the force required to fracture the hilum is higher than the adhesion force between the cantilever and the spore. Most attempts to increase the adhesion between the spore and the cantilever, and thus apply higher forces on the hilum, failed; probably because the wet spore surface does not allow strong bonding. However, numerous trials with cantilevers coated with poly-L-lysine yielded a few strongly bonded cantilevers. For these experiments, the hilum either ruptures for forces in the low range observed before or for large forces above 1 μN and up to 4.8 μN (Fig. 7). The two spore classes provide direct evidence for the development of an abscission zone at spore maturity to allow easy release of the spore (van Neil et al., 1972; McLaughlin et al., 1985). The upper force range gives an estimate of the force required to rupture the hilum before the abscission zone has fully developed.

For a finite rupture force, the spore velocity is reduced by an amount ΔV that depends on the work done to fracture the hilum. During the late phase of the coalescence process, the sterigma is stretched until the hilar region is fractured. Given a stiffness k and an elongation δ for the sterigma, the elastic force acting on the sterigma is $F_E=k\delta$. When F_E reaches F_B, the hilum breaks. The energy needed to sever the attachment is equal to the work done by the elastic deformation: $E_B=F_B^2/(2k)$. We measured k of the sterigma for different spores with the force experiment reported in Fig. 7 and found values between 0.45 N m^{-1} and 1.5 N m^{-1} (mean of 0.72 N m^{-1}). Using our measurements of rupture force and stiffness, we can compute the energy required to liberate the spores in *A. auricula*. The energy of fracture is $E_B=1.6\times10^{-14}$ J and corresponds to a velocity reduction of 3.4%. Therefore, the work of fracture dissipates only a small fraction of the kinematic energy of the spore. However, Buller's drop does not contain enough energy to rupture the hilum before the abscission zone has been weakened. This observation may explain why, on some occasion, fusion of Buller's drop fails to release the spore (Buller, 1909-1950).

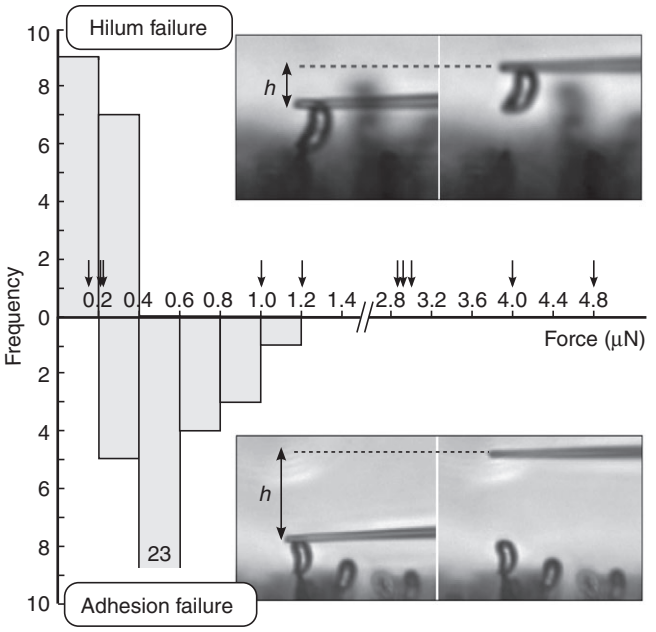

Fig. 7. Rupture force measurements. The abscissa gives the maximal force recorded at the time of failure, which involved either a fracture of the hilum (top histogram) or an adhesion failure between the spore and the pipette (bottom histogram). The distribution indicates two broad classes of spores: weakly attached spore with rupture force ≤0.4 μN and strongly attached spores that could not be detached with forces of up to 1.2 μN. Arrows indicate the hilum rupture force recorded in a second series of experiments with cantilevers coated with poly-L-lysine. The force is proportional to the displacement of the pipette (*h*) after fracture of the hilum or adhesion failure.

Transfer of surface energy

The central component of our model is the calculation of the surface energy available to accelerate the drop. This energy is equal to the difference in surface energy between the initial state just before coalescence and the final state just after fusion. The exact expression for the difference in energy depends on spore geometry and final drop geometry. For *A. auricula*, our observations of the coalescence process (Fig. 5) reveal that the fused drop adopts a geometry close to a spherical cap. The difference in surface energy is (see Materials and methods):

$$\Delta E_p = \gamma 4\pi R_D^2 (1 - R_D / R'_D). \quad (12)$$

This equation gives a measure of the energy available to accelerate the drop. Setting the drop kinetic energy ($m_D V_D^2/2$) equal to the freed

surface energy and using $m_D=4\pi\rho R_D^3/3$, we find for the drop velocity:

$$V_D \approx \left[\frac{6\gamma}{\rho}(1/R_D - 1/R_D')\right]^{1/2}. \quad (13)$$

The expression for V_D takes into account the spore geometry and wettability through R_D'. Using the conservation of momentum between the drop and spore, it is possible to predict the initial spore velocity V_0. The prediction for the ejection shown in Fig. 3A is $1.2\,m\,s^{-1}$ whereas the observed velocity is $0.8\,m\,s^{-1}$. The ratios of the predicted and observed velocities for the entire set of experiments are listed in Table 2. The predicted velocity is surprisingly accurate given that energy loss, either to break the hilum or through dissipation during the fusion process, has not been taken into account.

It is also possible to predict the angular velocity of the spore. A torque is exerted on the spore because the surface tension force is applied at some distance from the point of contact between the spore and the sterigma (Fig. 6A). This torque explains the rotation of the ejected spore. Using the conservation of angular momentum (Happel and Brenner, 1983), we have $m_D V_D l = m_{SD} r_g^2 \Omega_0$, where l is the distance between the global center of mass and the point of drop fusion. For the discharge shown in Fig. 3A, l=3 μm, giving a calculated angular velocity of $\Omega_0 < 8\times10^4\,rad\,s^{-1}$, in good agreement with the measured value of $9\times10^4\,rad\,s^{-1}$. We have not been able to investigate this aspect of the discharge further because the rotation of most spores was not confined to the imaging plane and thus could not be measured.

In the *Sporobolomyces* yeasts, the spore is nearly spherical and is covered by a film of water (Fig. 4). The fusion is thus close to the coalescence of a drop of radius R_D onto a perfectly wetting spherical spore of radius R_S. The difference in surface energy is then:

$$\Delta E_p = \gamma 4\pi (R_D^2 + R_S^2 - R_D'^2), \quad (14)$$

where $R_D'=(R_D^3+R_S^3)^{1/3}$. Equating the surface energy and the drop kinetic energy and solving for the drop velocity, we find:

$$V_D \approx \left[\frac{6\gamma}{\rho R_D^3}(R_D^2 + R_S^2 - R_D'^2)\right]^{1/2}. \quad (15)$$

Using this equation and the conservation of momentum, we predict a velocity V_0=3.4 $m\,s^{-1}$ whereas the observed velocity is 2.3 $m\,s^{-1}$. Given that some energy is necessarily lost in the coalescence process and in breaking the hilum, the agreement is again very good.

A test of the model

The key assumption of our model is that the drop reaches a characteristic velocity V_D that can be predicted from the change in surface energy of the system. To test the validity of this assumption, we performed experiments on an artificial system that mimics the fusion of Buller's drop. A drop was placed on a highly hydrophobic plate while another plate, this one wettable, was approached slowly from above until it touched the drop. Contact with the wettable plate induced a fast upward motion of the drop (Fig. 8). The contrast of wettability between the two substrates was such that the drop moved in its entirety from the lower surface to the upper one. This coalescence process is very similar to what happens when a drop wets the spore. Biance et al. performed a similar experiment but with plates of similar wettability, leading to a final state where the drop is split between the two surfaces (Biance et al., 2004). They provided a scaling relationship for the horizontal growth dynamics of the neck. Here, we complement their analysis with a study of the vertical motion of the center of mass.

We found that after a brief acceleration, the drop's center of mass moves upward at a constant speed (Fig. 8H). Therefore, the fusion process is associated with a characteristic velocity of the center of mass. We measured this characteristic velocity in a series of experiments and plotted it as a function of the theoretical velocity predicted from Eqn 13 (Fig. 8I). The observed drop velocity is

Table 2. Ratio of the measured (V_0) and predicted ($\hat{V}_0$) initial spore velocity

Species	$V_0/\hat{V}_0$	σ	*N*
Auricularia	0.73	0.13	5
Sporobolomyces	0.68	0.12	5
Drop-plane system*	0.28	0.02	11

Mean values are reported with their standard deviations (σ) and sample size (*N*). *Based on the ratio of the observed and predicted drop velocities.

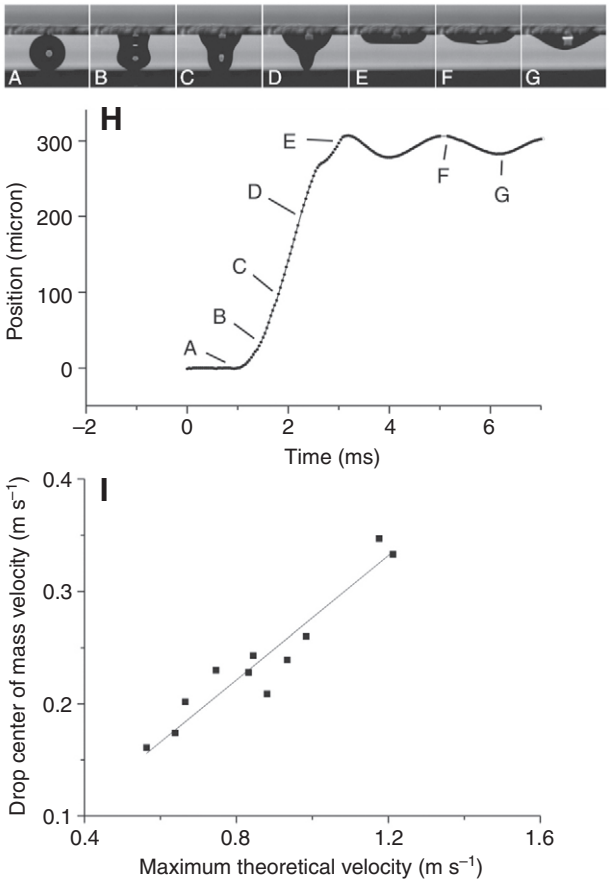

Fig. 8. Coalescence of a drop (R_D=400 μm) onto a wettable plate. (A–G) Image sequence of the coalescence process. (H) The position of the drop's center of mass is plotted as a function of time. The letters correspond to the frames above. (I) Velocity of the drop center of mass as a function of the predicted velocity $V_D=[(6\gamma/\rho)(1/R_D-1/R_D')]^{1/2}$. The slope of the relationship is β=0.28 (R=0.95). R_D, R_D', radius of the drop before and after fusion, respectively. V_D, velocity of the drop; γ, surface tension; ρ, density of the object.

proportional to the predicted velocity, with a proportionality constant β=0.28. The parameter β is a measure of the efficiency of the transfer of surface energy to kinetic energy. The value of β below one indicates that a fraction of the surface energy is lost in the coalescence process and therefore not available to accelerate the drop. By the same token, we can interpret the velocity ratios listed in Table 2 as a measure of the efficiency of the energy transfer in the ballistospores. *Auricularia auricula* and the *Sporobolomyces* yeasts show a similar efficiency with more than two third of the surface energy liberated contributing to the kinetic energy of the spore.

DISCUSSION

The use of surface tension by ballistosporic fungi offers a new paradigm for performing work at the micron scale. One clear advantage of this mechanism is that work, being performed by the fusion of a water droplet, comes virtually for free. It is only under this condition that the innumerable spores contained in a mushroom cap can all be equipped with their own discharge apparatus. The ballistosporic mode of dispersal is in sharp contrast with the mass release of spores or propagules by specialized launching structures found in other taxa (Straka, 1962). It is therefore of great interest to uncover the design principles that make surface tension an effective source of energy.

As first stated by Ingold (Ingold, 1939), the key step for ballistospore release is the transfer of surface energy stored in Buller's drop to the spore. Our analysis emphasizes the critical role played by the sterigma. First, during the early phase of the coalescence process, the sterigma provides the external force that prevents the spore from moving toward the drop. The global center of mass of the spore–drop complex is thus projected forward leading to ejection. In the late phase of the coalescence process, the sterigma is now put under tension and should fracture easily to prevent dissipation of the spore energy. Our measurements of the force required to release the spore from the sterigma show that an active weakening of the hilum takes place before ejection. The characteristic rupture force of 0.15 μN (N=15) recorded for a weakened hilum is comparable with the rupture force of 0.1 μN reported for wind-dispersed fungal conidiospores (Aylor, 1975). This value is large compared with the gravitational force acting on the spore ($F_g<2\times10^{-6}$ μN) but small compared with the surface tension force that can be exerted by a drop at this scale ($F_\gamma=\gamma 2\pi R_D<1.4$ μN, where R_D=2.25 μm is the drop radius). However, a force of up to 4.8 μN is necessary to detach an unweakened spore (Fig. 7), i.e. three times the surface tension force. Therefore, without an active weakening mechanism, spore ejection would be impossible.

To predict the initial velocity of the spore, we developed a model that focuses on the surface energy freed during the coalescence process. This model predicts with surprising accuracy the initial translational and angular velocity of the spore, particularly if one makes allowance for energy dissipation during fusion. A prediction of the model is that the geometry of the fused drop affects the amount of energy available to eject the spore. Consequently, spore morphology and the wetting properties of the spore surface can play an important role in the transfer of surface energy to kinetic energy. The low efficiency of energy transfer in our artificial system when compared with ballistospores (Table 2) also emphasizes the challenges associated with the fine-tuning of such a mechanism. It is likely that the difference in scale between the two systems explains the higher efficiency for ballistospore ejection. It is also noteworthy that our model predicts similar efficiency of energy transfer for the two species studied despite differences in spore geometry and a threefold difference in the initial velocity between the *Sporobolomyces* and *A. auricula* spores.

A way to evaluate viscous loss is to calculate the energy loss in volume during the fusion process. This energy is $E_V=T_D\mu\int\xi^2 dV$, where $T_D\sim R_D/V_D$ is the characteristic time for the drop merging process and ξ is the shear rate. By taking a characteristic shear rate $\xi\sim V_D/R_D$ due to the small deformation of the drop, the integration gives $E_V\approx 4\pi\mu R_D^2 V_D/3$. Hence, the ratio between viscous energy loss and the surface energy of the drop is: $E_V/E_p=E_V/4\pi\gamma R_D^2=\mu V_D/3\gamma=Ca/3=1/20$. The energy ratio corresponds to the capillary number (Ca). Here, this ratio is much smaller than one, indicating small viscous loss.

We have found it useful to compare ballistospore release with jumping in animals. We first note that the take-off velocity of the spore (1–2 m s^{-1}) falls precisely within the narrow range of take-off velocities (1–4 m s^{-1}) reported for good jumpers from insects to mammals (Vogel, 2005a; Vogel, 2005b). This striking observation suggests that a take-off velocity on the order of 1 m s^{-1} is a fundamental limit for jumpers whether they achieve this velocity through muscle work or surface tension. Vogel (Vogel, 2005b) posited that the strength of biomaterials may impose limits on the stress that can be applied to accelerate jumpers and thus may set the maximal take-off velocity. However, it is doubtful that the same argument would apply to ballistospores. As we have shown, the surface tension force exerted by Buller's drop is F_γ=1.4 μN and is applied on a cross-section of 5 μm^2, which is a level of stress that most biomaterials can sustain.

In both insects and vertebrates, the velocity of the center of mass is known to increase monotonically during the active part of the jump up to the take-off velocity (Burrows, 2006; Burrows, 2008; Marsh and Johnalder, 1994). The evolution of the center of mass velocity can be accounted for if a finite force is applied during the entire hind limb deployment. By analogy, it would be tempting to assume that the velocity of Buller's drop in ballistospores follows a similar evolution with surface tension, instead of muscle work, providing a roughly constant force over the entire distance traveled by the drop. However, as can be seen in our artificial system (Fig. 8H), this approach would lead to a gross overestimate of the drop velocity. The drop is in fact accelerated over a very short distance and then displaced at a constant characteristic velocity. We have argued that understanding what sets this characteristic velocity is the key to predicting the spore velocity at ejection. Our results show that the characteristic velocity scales with the surface energy freed during the coalescence (Fig. 8I) and thus highlight the importance, in ballistospores, of the final geometry of Buller's drop in determining the energy available for discharge and the take-off velocity of the spore.

LIST OF SYMBOLS

A_D	drop surface area after fusion
A_S	area of the spore covered by the drop after fusion
a	acceleration of the spore
a, b	minor and major semi-axes of the spheroid
Ca	capillary number
D	drag force
E_B	energy of fracture
E_K	translational kinetic energy
E_R	rotational kinetic energy
E_V	energy loss in volume
F_B	rupture force of the hilum
F_D	force applied by the drop
F_E	elastic force
F_g	force of gravity

F_γ	surface tension force
F_R	ground reaction force
F_S	force applied by the spore
F_{SD}	force applied by the spore–drop complex
F_{St}	force applied by the sterigma
g	gravitational acceleration
k	stiffness
L_S	length of the spore
l	distance between the global center of mass and the point of drop fusion
M	moment at the joints
m	mass
m_D	mass of the drop
m_{SD}	mass of the spore–drop complex
R	mean radius
R_D	radius of the drop before fusion
R_D^t	radius of the drop after fusion
Re	Reynolds number
r_g	spore's radius of gyration
R_S	spherical spore radius
t	time
T_D	characteristic time for drop coalescence
V_0	initial spore velocity
V_D	velocity of the drop
W_S	width of the spore
v	velocity
x	axis of discharge
γ	surface tension at liquid–vapor interface
γ_{SL}	surface tension at spore–liquid interface
γ_{SV}	surface tension at spore–vapor interface
ΔE_p	surface energy freed during the fusion process
δ	elongation
θ	angular position of the spore
θ	contact angle
μ	dynamic viscosity of air
ν	kinematic viscosity of air
ξ	shear rate
ρ	density
τ_R	characteristic decay time associated with angular velocity
τ_T	characteristic decay time associated with the translational velocity
Ω_0	initial angular velocity

We would like to thank the MRSEC at Harvard University and D.A. Weitz for funding; B. Roman, L. Mahadevan, D. Quéré, and H. A. Stone for useful comments on the manuscript; as well as D. H. Pfister, N. M. Holbrook and M. A. Zwieniecki for help with the experiments.

REFERENCES

Aylor, D. E. (1975). Force required to detach conidia of *Helminthosporium maydis*. *Plant Physiol.* **55**, 99-101.
Biance, A., Clanet, C. and Quéré, D. (2004). First steps in the spreading of a liquid droplet. *Phys. Rev. E* **69**, 016301.
Buller, A. (1909-1950). *Researches on Fungi*, vols. 1-7. London: Longmans, Green and Company.
Burrows, M. (2006). Jumping performance of froghopper insects. *J. Exp. Biol.* **209**, 4607-4621.
Burrows, M. (2008). Jumping in a wingless stick insect, *Timema chumash* (phasmatodea, timematodea, timematidae). *J. Exp. Biol.* **211**, 1021-1028.
de Gennes, P., Brochard-Wyart, F. and Quéré, D. (2003). *Capillarity and Wetting Phenomena: Drops, Bubbles, Pearls, Waves*. New York: Springer Verlag.
Happel, J. and Brenner, H. (1983). *Low Reynolds Number Hydrodynamics*. New York: Springer Verlag.
Ingold, C. (1939). S*pore Discharge in Land Plants*. Oxford: Oxford University Press.
Marsh, R. L. and Johnalder, H. B. (1994). Jumping performance of hylid frogs measured with high-speed cine film. *J. Exp. Biol.* **188**, 131-141.
McLaughlin, D., Beckett, A. and Yoon, K. (1985). Ultrastructure and evolution of ballistosporic basidiospores. *Bot. J. Linn. Soc.* **91**, 253-271.
Money, N. (1998). More g's than the space shuttle: ballistospore discharge. *Mycologia* **90**, 547-558.
Pringle, A., Patek, S., Fischer, M., Stolze, J. and Money, N. (2005). The captured launch of a ballistospore. *Mycologia* **97**, 866-871.
Straka, H. (1962). *Handbuch der Planzenphysiologie, Volume 17: Nicht durch Reize ausgelöste Bewegungen*, pp. 716-835. Berlin: Springer Verlag.
Turner, J. and Webster, J. (1991). Mass and momentum transfer on the small scale: how do mushrooms shed their spores? *Chem. Eng. Sci.* **46**, 1145-1149.
van Neil, C., Garner, G. and Cohen, A. (1972). On the mechanism of ballistospore discharge. *Arch. Mikrobiol.* **84**, 129-140.
Vogel, S. (2005a). Living in a physical world. II. The bio-ballistics of small projectiles. *J. Biosci.* **30**, 167-175.
Vogel, S. (2005b). Living in a physical world. III. Getting up to speed. *J. Biosci.* **30**, 303-312.
Webster, J., Davey, R., Smirnoff, N., Fricke, W., Hinde, P., Tomos, D. and Turner, J. (1995). Mannitol and hexoses are components of Buller's drop. *Mycol. Res.* **99**, 833-838.